

Long-Term Adult Feline Liver Organoid Cultures for Disease Modeling of Hepatic Steatosis

Hedwig S. Kruitwagen,^{1,*} Loes A. Oosterhoff,¹ Ingrid G.W.H. Vernooij,¹ Ingrid M. Schroll,¹ Monique E. van Wolferen,¹ Farah Bannink,¹ Camille Roesch,¹ Lisa van Uden,¹ Martijn R. Molenaar,² J. Bernd Helms,² Guy C.M. Grinwis,³ Monique M.A. Versteegen,⁴ Luc J.W. van der Laan,⁴ Meritxell Huch,^{5,6} Niels Geijsen,^{1,5} Robert G. Vries,⁵ Hans Clevers,⁵ Jan Rothuizen,¹ Baukje A. Schotanus,¹ Louis C. Penning,¹ and Bart Spee¹

¹Department of Clinical Sciences of Companion Animals, Faculty of Veterinary Medicine

²Department of Biochemistry and Cell Biology, Faculty of Veterinary Medicine & Institute of Biomembranes Utrecht University, 3584 CM Utrecht, the Netherlands

³Department of Pathobiology, Faculty of Veterinary Medicine, Utrecht University, 3584 CL Utrecht, the Netherlands

⁴Department of Surgery, Erasmus MC-University Medical Center, 3000 CA Rotterdam, the Netherlands

⁵Hubrecht Institute, University Medical Centre, Utrecht University, 3584 CT Utrecht, the Netherlands

⁶Present address: Department of Physiology, Development and Neuroscience, Wellcome Trust/Cancer Research UK Gurdon Institute, Wellcome Trust/MRC Stem Cell Institute, University of Cambridge, Tennis Court Road, CB2 1QN Cambridge, UK

*Correspondence: h.s.kruitwagen@uu.nl

<http://dx.doi.org/10.1016/j.stemcr.2017.02.015>

SUMMARY

Hepatic steatosis is a highly prevalent liver disease, yet research is hampered by the lack of tractable cellular and animal models. Steatosis also occurs in cats, where it can cause severe hepatic failure. Previous studies demonstrate the potential of liver organoids for modeling genetic diseases. To examine the possibility of using organoids to model steatosis, we established a long-term feline liver organoid culture with adult liver stem cell characteristics and differentiation potential toward hepatocyte-like cells. Next, organoids from mouse, human, dog, and cat liver were provided with fatty acids. Lipid accumulation was observed in all organoids and interestingly, feline liver organoids accumulated more lipid droplets than human organoids. Finally, we demonstrate effects of interference with β -oxidation on lipid accumulation in feline liver organoids. In conclusion, feline liver organoids can be successfully cultured and display a predisposition for lipid accumulation, making them an interesting model in hepatic steatosis research.

INTRODUCTION

A specific adult liver stem cell population acting as second line of defense in liver regeneration has been described in several species, including rodents, humans, canines, and felines (Wang et al., 2003; Roskams et al., 2003; Kruitwagen et al., 2014; Ijzer et al., 2009). Recently, a three-dimensional and highly proliferative organoid culture system was developed for mouse, human, and dog liver stem cells (Huch et al., 2013, 2015; Nantasanti et al., 2015). Liver organoids have been proposed as in vitro disease-modeling tool for several genetic liver diseases, such as α 1-antitrypsin deficiency, Alagille syndrome, and canine copper storage disease (Huch et al., 2013, 2015; Nantasanti et al., 2015). However, many liver diseases do not have monogenetic etiology and have a more complex pathophysiology. We aimed to explore the potential of liver organoids to model non-genetic metabolic liver disease.

One of the most common metabolic liver diseases in humans is liver steatosis, also known as non-alcoholic fatty liver disease (NAFLD) (Younossi et al., 2016). Interestingly, a severe type of hepatic steatosis also occurs in cats (feline hepatic lipidosis, FHL) (Center et al., 1993). Both in human

and feline steatosis, hepatocyte lipid overload arises from an increased amount of free fatty acids (FFA) that are offered to the liver, and obesity and insulin resistance are known risk factors for its development (Center, 2005; Cohen et al., 2011). NAFLD can result in hepatocyte degeneration and inflammation (non-alcoholic steatohepatitis), and ultimately in excessive liver fibrosis and hepatocellular carcinoma (Cohen et al., 2011).

We asked whether liver organoids could be used to model hepatic steatosis and if so, whether there would be species differences in hepatocyte lipid-handling capacity. We hypothesized that liver cells from cats could have pronounced lipid accumulation properties. For this purpose, a culture system of feline liver progenitor cells as three-dimensional organoids was established from cat liver samples. First, we describe the isolation, long-term culture, and characterization of feline liver organoids. Second, we investigate the potential of liver organoids to model hepatic steatosis and compare lipid accumulation capacity between organoids of mouse, human, dog, and cat liver. Third, as proof of principle we show the effects of interference with β -oxidation on lipid accumulation and viability in feline liver organoids.



RESULTS

Establishment of the Feline Liver Organoid Culture

Organoids were successfully cultured from cat liver samples of different origin (i.e., fresh, frozen, and fine-needle aspirate [FNA]) (Figure 1A). Biliary duct fragments were observed in the supernatant after digestion (Figure 1B). After 3–6 days in culture, spherical structures appeared with occasional folding and budding. Morphology and passage rate were similar between donors and tissue sources. It was even possible to culture organoids from an undigested FNA plated straight into Matrigel; organoids appeared after 5 days, emerging from the remnant liver tissue fragments (Figure 1C). Organoid morphology remained similar between passages (p1 to p25, Figure 1D). Feline liver organoids could be cultured in expansion medium as published for mouse, dog, and human liver organoids with varying success rates on short- and long-term culture (Figure S1) (Huch et al., 2013, 2015; Nantasanti et al., 2015). However, a hybrid medium (hereafter named cat expansion medium) performed best and allowed for a high split ratio (1:11) in long-term culture. It was possible to cryopreserve feline liver organoids as fragments, which formed organoids again upon thawing.

Characterization of Feline Liver Organoids

We observed feline liver organoids microscopically as spherical structures with occasional folding and intraluminal epithelial projections (Figure 2A). They were composed of single-layered cubical epithelium and stained positive for the epithelial marker E-cadherin (Figure 2A). When pulsed with 5-ethynyl-2'-deoxyuridine (EdU) for 6 hr, 16.4% ± 8.1% of organoid nuclei had incorporated the thymidine analog (S phase of cell cycle, representative image shown in Figure 2A). Gene expression analysis indicated that feline liver organoids expressed adult stem cell markers *LGR5*, *PROM1*, and *BMI1* (Figure 2B). Feline liver organoids expressed hepatic progenitor cell/biliary markers *KRT7* (Ijzer et al., 2009), *KRT19*, and *HNF1β*, as well as early hepatocyte specification markers *HNF4α* and *TBX3* and very low levels of *ALB*. Genes of mature hepatocyte markers *PROX1*, *PC*, *HMGCL*, *TTR*, *FAH*, and *CYP3A132* were expressed but at low levels compared with normal cat liver. Gene expression patterns remained stable throughout the culture. At protein level, feline liver organoids were 100% positive for K19 (strong cytoplasmic staining), HNF1β (moderate to strong nuclear staining), and self-renewal marker BMI1 (moderate to strong nuclear staining) (Figure 2C). Feline liver organoids were mainly negative for albumin immunoreactivity, but in many organoids a weak cytoplasmic staining was observed in small clusters of cells within single organoids. All organoids were negative for mature hepatocyte marker HepPar-1. Feline liver organoids

were mainly negative for ZO1, but in some organoids a weak membranous staining was observed in small clusters of cells within single organoids. Metaphase spread analysis showed a normal chromosome count in low and high passages, indicating long-term genetic stability of the cells similarly to liver organoids from other species (Figure 2D; Huch et al., 2013, 2015; Nantasanti et al., 2015).

Differentiation of Organoids toward Hepatocyte-like Cells

Upon culture in differentiation medium, gene expression of mature hepatocyte markers *FAH*, *CYP3A132*, and *TTR* increased compared with expansion-medium conditions, while expression of adult stem cell marker *LGR5* decreased (Figure 3A). Keratin-19 immunoreactivity changed from a strong cytoplasmic to a moderate membranous staining, indicative of an “intermediate hepatocyte” phenotype (Figure 3B; Roskams et al., 2004). BMI1 immunoreactivity changed from a moderate-strong nuclear staining in expansion-medium conditions to a weak nuclear staining in differentiation-medium conditions. ZO1 staining increased in differentiated feline liver organoids, as more cells were positive in differentiation-medium compared with expansion-medium conditions. Organoids in differentiation medium, but not in expansion medium, accumulated glycogen as indicated by positive PAS staining. HepPar1 staining was not observed upon differentiation (data not shown). Proliferation ceased abruptly after switching organoids from expansion medium to differentiation medium (Figure 3C). Hepatocyte function testing revealed increased aspartate aminotransferase levels, albumin secretion into the medium, and CYP450 activity in organoids in differentiation-medium conditions compared with expansion-medium conditions (Figure 3D).

Feline Liver Organoids for Disease Modeling of Hepatic Steatosis

To investigate liver organoids as a potential in vitro model for steatosis, we mimicked circumstances of excess FFA concentrations and measured intracellular lipid accumulation with the lipophilic dye LD540 using flow cytometry (Figure S2). We compared organoids from mouse, human, dog, and cat liver (four donors each) to assess species differences in lipid accumulation capacity. Median fluorescence intensity of LD540 was quantified in liver organoid cells after either control (BSA) or FFA treatment. For all four species, an increase in LD540 median fluorescence intensity was observed after FFA treatment compared with control, indicating intracellular lipid accumulation (Figure 4A). When this increase was compared between species, cat liver organoids showed more lipid accumulation than human liver organoids after FFA treatment (192 ± 104 versus 61 ± 36, $p = 0.029$). LD540-positive intracellular lipid droplets

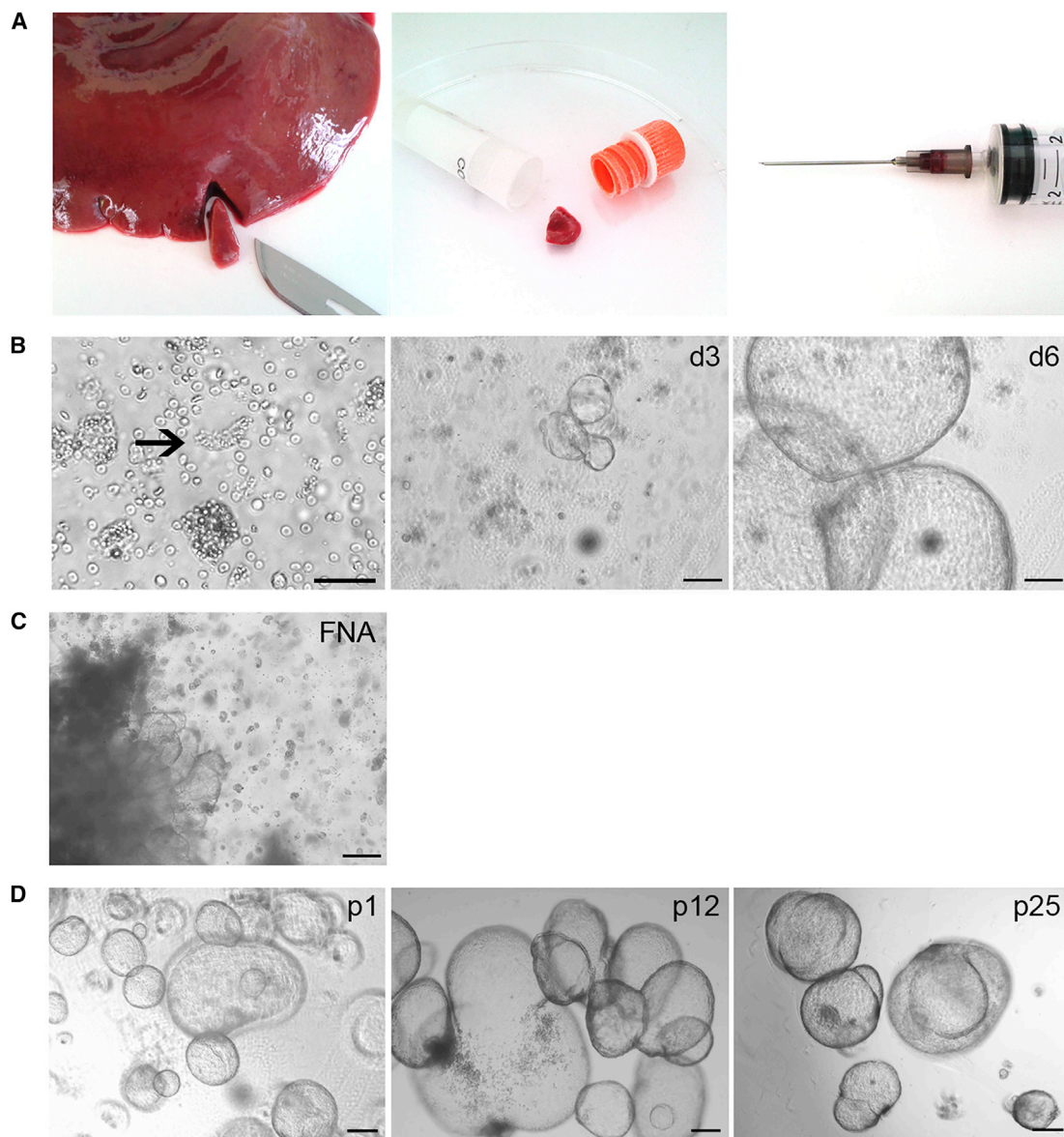


Figure 1. Establishment of an Organoid Culture from Feline Liver Samples

(A) Fresh and snap-frozen liver samples (wedge biopsies of 5 mm³) could be used with equal success rate to establish an organoid culture. It was also possible to start a feline liver organoid culture from a fine-needle aspirate (aspirate visible in the conus of the needle).

(B) Representative phase-contrast images of duct isolation and organoid culture. After enzymatic digestion of feline liver samples, biliary duct fragments (arrow) were observed (scale bar represents 50 μm). Ducts were cultured in Matrigel and defined medium. After approximately 3 days in culture (d3), spherical structures appeared that rapidly grew out to large organoids within 6 days (d6) (scale bars represent 100 μm).

(C) Representative phase-contrast image of an undigested fine-needle aspirate (FNA) plated straight into Matrigel. After 5 days, organoids emerged from the remnant liver tissue fragments. Scale bar represents 100 μm.

(D) Representative phase-contrast images of feline liver organoids in early, medium, and late passages (p1, p12, and p25). Morphology remained similar during long-term culture. Scale bars represent 100 μm.

See also [Figure S1](#).

were visualized in whole-mount immunofluorescent stainings of mouse, human, dog, and cat liver organoids after FFA treatment (representative images shown in [Figure 4B](#)).

Transcriptional analysis of human and cat liver organoids treated with FFA indicated that in both species *PLIN2* was upregulated, consistent with increased lipid-droplet

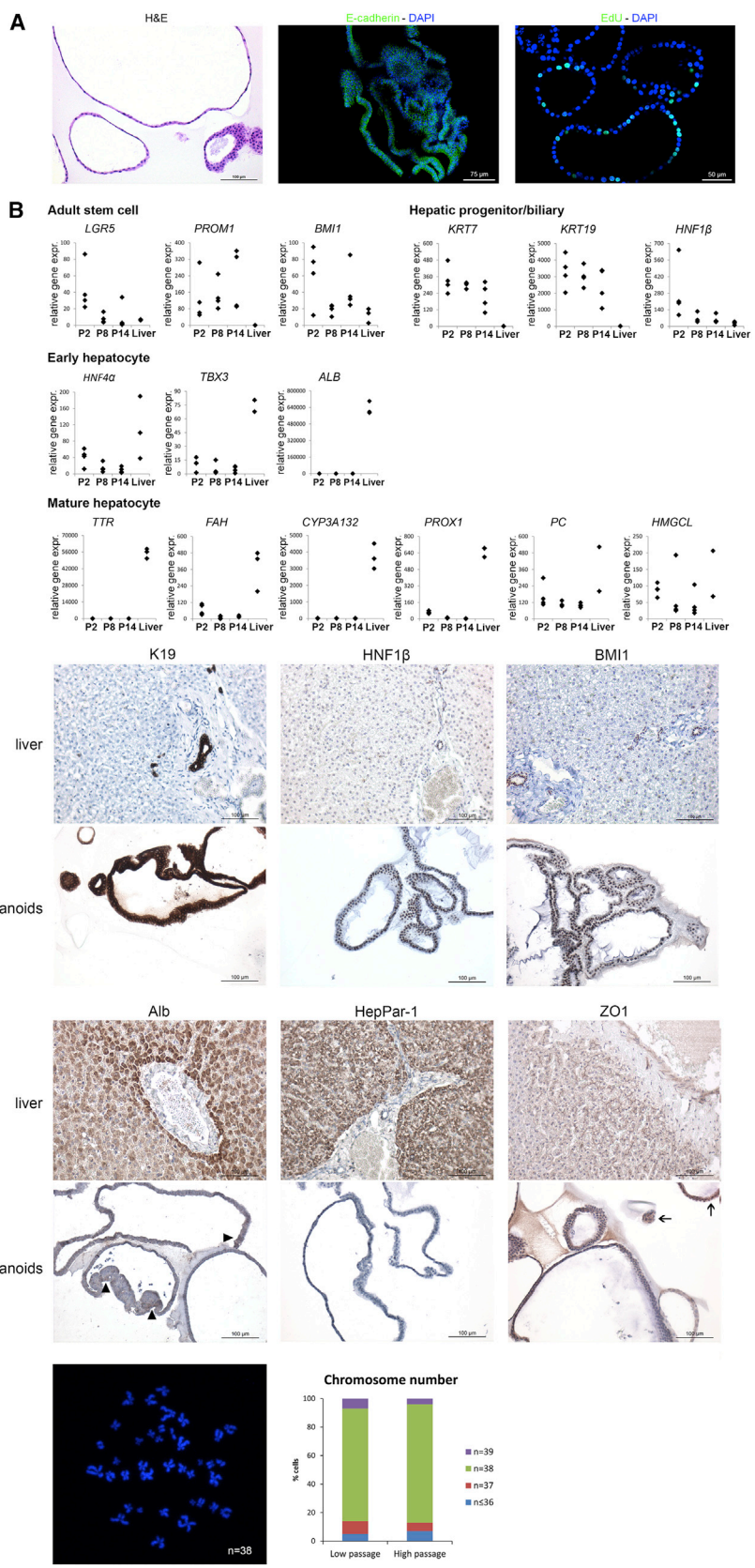


Figure 2. Characterization of Feline Liver Organoids

(A) Representative cytological and immunofluorescent images of feline liver organoids. H&E staining showed that organoids consisted of single-layered cubical epithelium. They stained positive for epithelial marker E-cadherin (green) and were highly proliferative in culture as shown by EdU staining (green, marks S phase of the cell cycle). DAPI (blue) was used as nuclear counterstain.

(B) Gene expression analysis of feline liver organoids (n = 4 donors) in different passages (p2, p8, p14) and normal cat liver. Relative gene expression (expr.) is shown of adult stem cell, progenitor/biliary, and early and mature hepatocyte markers.

(C) Representative images of immunocyto- and histochemical stainings of feline liver organoids and normal cat liver. Organoids stained positive for progenitor/biliary markers K19, HNF1β, and BMI1. They stained negative for hepatocyte marker HepPar-1, but for albumin and ZO1 small clusters of cells within single organoids stained positive (indicated by arrowheads and arrows, respectively).

(D) Karyotyping of feline liver organoids. A representative metaphase spread is shown of a cell with a normal chromosome number (n = 38). Chromosome counts were compared between low- and high-passage number cultures (p3–p7 versus p16–p23, n = 4 donors per category) and plotted as percentage of cells with a normal chromosome number (n = 38), one gain (n = 39), one loss (n = 37), or two or more losses (n ≤ 36).

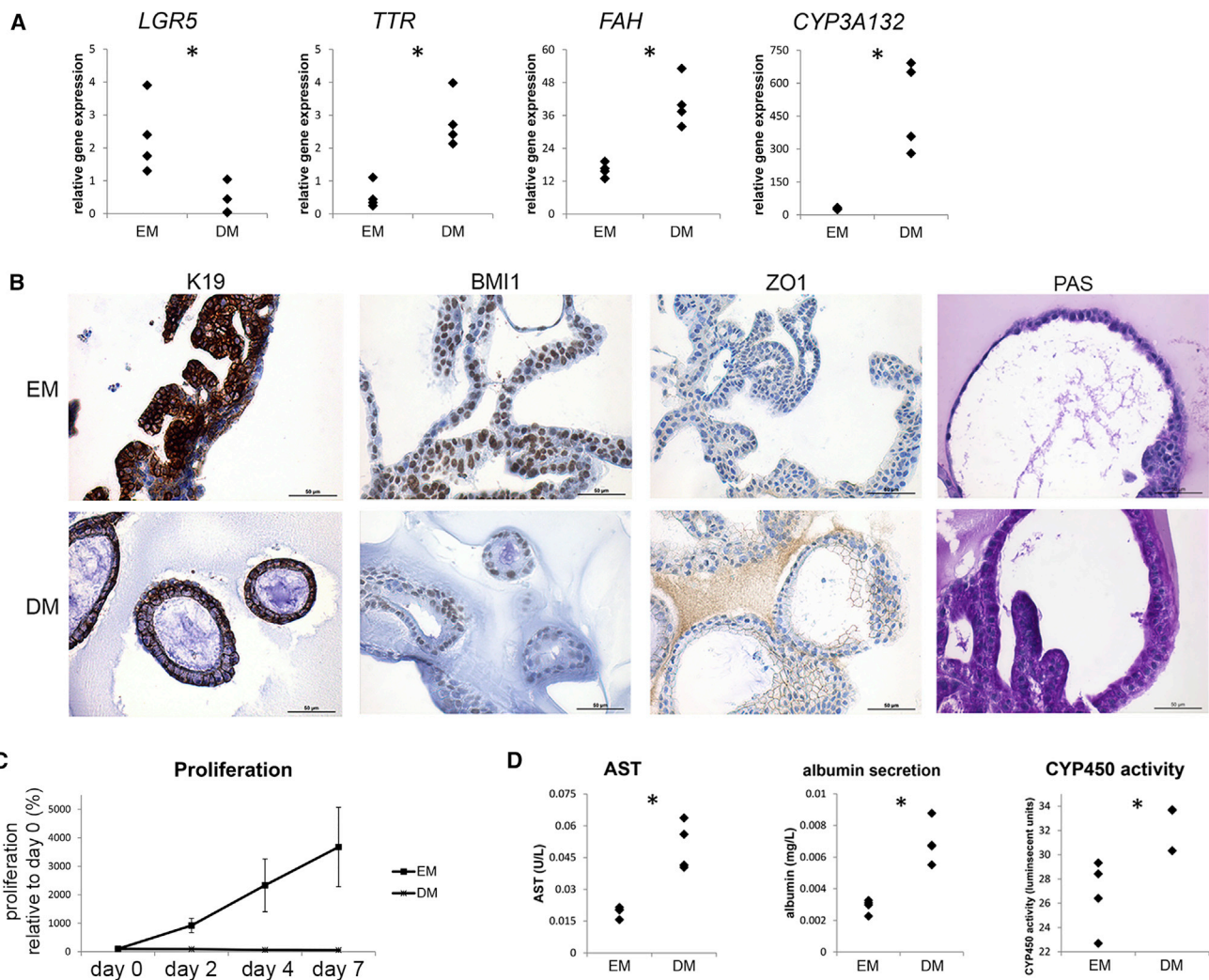


Figure 3. Differentiation of Feline Liver Organoids toward Hepatocyte-like Cells

(A) Relative gene expression of feline liver organoids cultured in expansion medium (EM) and differentiation medium (DM) ($n = 4$ donors). * $p < 0.05$, Mann-Whitney U test.

(B) Representative images of immunocytochemical stainings for K19, BMI1, and ZO1 and PAS staining (indicating glycogen accumulation) of feline liver organoids cultured in EM and DM.

(C) Growth curve derived from an Alamar blue assay of feline liver organoids cultured in EM and DM for 7 days ($n = 4$ donors). Proliferation is presented as percentage relative to measurement at day 0. Error bars indicate SD.

(D) Hepatocyte function tests of feline liver organoids cultured in EM and DM ($n = 4$ donors). Aspartate aminotransferase (AST) levels, albumin secretion in the medium, and CYP450 activity were corrected for cell input with Alamar blue. * $p < 0.05$, Mann-Whitney U test.

formation (Figures 4C and S3). *SREBF1*, a transcription factor that induces de novo lipogenesis, was decreased in human and feline organoids. FFA-treated feline organoids increased their expression of *CPT1A* (a key enzyme in β -oxidation) and *PPARG*, a transcription factor known to enhance β -oxidation. Both genes were unchanged in human organoids. In human organoids, FFA treatment decreased expression of *PPARA* and its downstream targets *ACADSB* and *AGPAT2*. Next, we studied the effects of either etomoxir or L-carnitine supplementation compared with

FFA treatment alone on lipid accumulation and viability in feline liver organoids. Etomoxir, a carnitine palmitoyl-transferase-1 inhibitor, blocks the transfer of FFA over the mitochondrial membrane (carnitine shuttle), preventing them from entering β -oxidation. Conversely, L-carnitine is an essential co-factor for the carnitine shuttle. In feline liver organoids, FFA treatment decreased viability of the cells compared with BSA control ($86\% \pm 2\%$ versus $96\% \pm 2\%$, $p = 0.034$) (Figure 4D); morphologically, the organoids gained a dark appearance (Figure 4E). Lipid accumulation

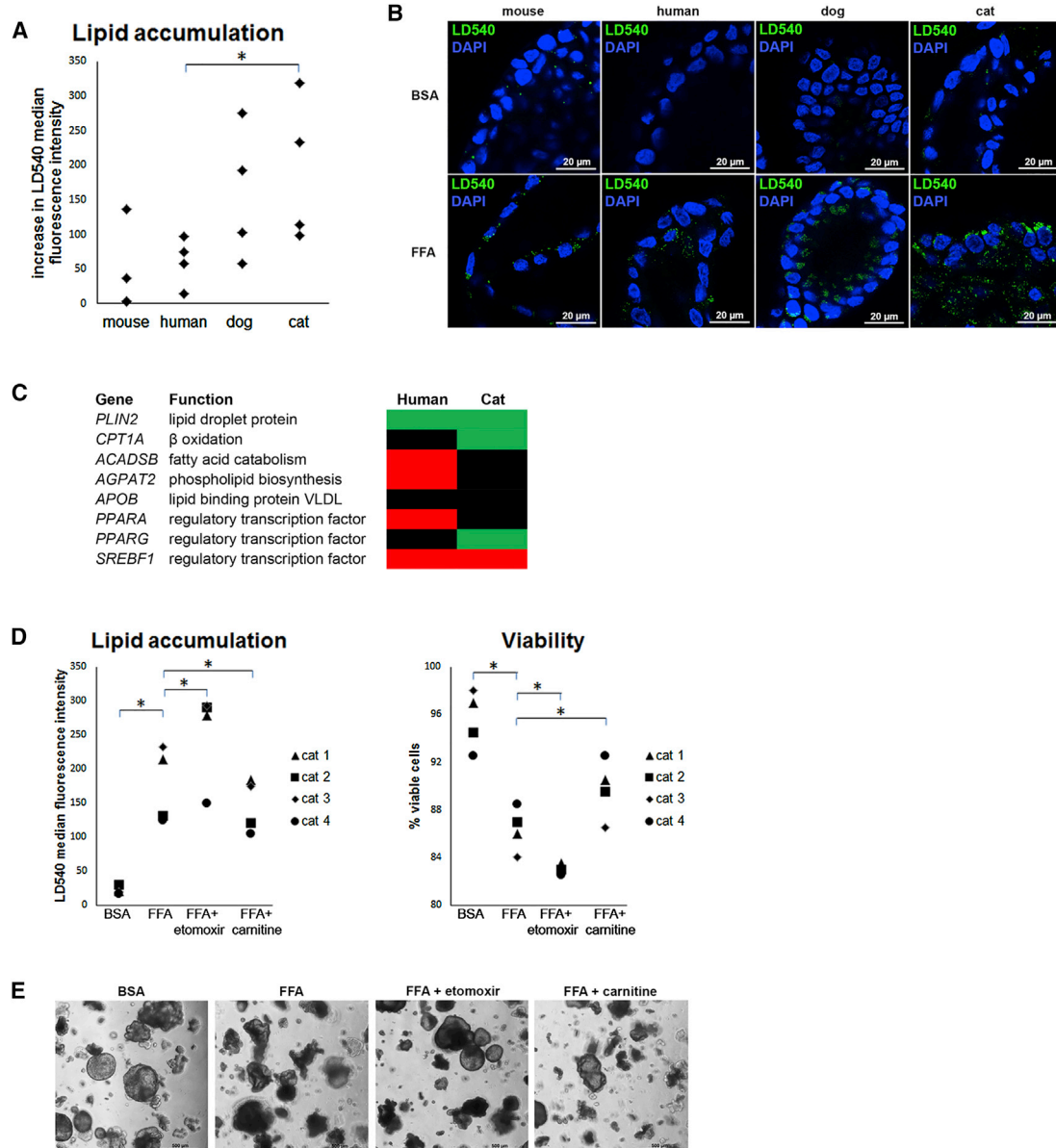


Figure 4. Liver Organoids for Disease Modeling of Hepatic Steatosis

(A) Lipid accumulation in liver organoids from mouse, human, dog, and cat ($n = 4$ donors per species). Intracellular lipids were stained with LD540 and fluorescence was quantified using flow cytometry (see also Figure S2). Data are presented as a dot plot and indicate the increase in LD540 median fluorescence intensity after free fatty acid (FFA) treatment compared with control treatment with BSA. $*p < 0.05$, Mann-Whitney U test.

(B) Representative immunofluorescent images of LD540 staining of mouse, human, dog, and cat liver organoids after control treatment (BSA) and FFA treatment. Intracellular lipid droplets stain green, nuclei are counterstained with DAPI (blue).

(C) Heatmap representing the transcriptional analysis of human and cat liver organoids treated with FFA compared with control treatment (BSA). Red indicates decreased gene expression, black unchanged gene expression, and green increased gene expression. See also Figure S3.

(D) Lipid accumulation in feline liver organoids treated with control (BSA), FFA, FFA plus etomoxir, and FFA plus L-carnitine. Intracellular lipid accumulation (left) was quantified with flow cytometry and plotted as LD540 median fluorescence intensity for each individual donor (cats 1, 2, 3, 4; $*p < 0.05$, Wilcoxon signed-rank test). Cellular viability after treatment (right) was measured using a trypan blue assay ($*p < 0.05$, Wilcoxon signed-rank test).

(E) Representative phase-contrast images of feline liver organoids treated with control (BSA), FFA, FFA plus etomoxir, and FFA plus L-carnitine.



increased with the FFA + etomoxir combination compared with FFA treatment alone (253 ± 69 versus 176 ± 56 , $p = 0.034$), and organoid viability decreased ($82\% \pm 3\%$ versus $86\% \pm 2\%$, $p = 0.034$). On the other hand, lipid accumulation decreased with FFA + carnitine supplementation compared with FFA treatment alone (146 ± 39 versus 176 ± 56 , $p = 0.034$), with an increase in organoid viability ($90\% \pm 3\%$ versus $86\% \pm 2\%$, $p = 0.034$). The morphology of the organoids treated with FFA + carnitine was more comparable with the BSA control than with the FFA-treated organoids, indicating that L-carnitine may help alleviate the surplus.

DISCUSSION

In the present study, long-term genetically stable feline liver organoid cultures were established and extensively characterized. To our knowledge, the liver organoids described in this study are the only available primary non-transformed long-term cell culture system from cats.

Feline liver organoids retain characteristics similar to liver organoids of other species, including massive proliferative capacity, an epithelial nature, and their gene expression pattern (Huch et al., 2013, 2015; Nantasanti et al., 2015). Feline liver organoids were positive for progenitor/biliary markers as well as early hepatocyte specification markers, indicative of a hepatic progenitor cell phenotype (Roskams et al., 2003). In addition, in some parts or cell clusters within single organoids albumin or ZO1 was expressed, whereas the rest of the structure was negative, indicating that there are different maturation levels within an organoid. This has also been described for mouse small intestinal organoids, which harbor a crypt and villus domain representative of a stem cell pool and a more mature progeny, respectively (Sato et al., 2009).

Feline liver organoid differentiation was associated with an abrupt cease in proliferation, a phenomenon also observed in cultures of primary hepatocytes, which cannot be expanded and rapidly dedifferentiate in vitro (Fraczek et al., 2013). Although feline liver organoids showed a higher expression of liver-specific genes and had increased albumin secretion and aspartate aminotransferase and CYP3A activity upon differentiation, they did not reach full maturation (e.g., they remained negative for HepPar-1). Until now it has not been possible to accomplish full hepatocyte maturation in vitro from an immature cell type, such as embryonic stem cells or induced pluripotent stem cells (Ochiya et al., 2010; Zhang et al., 2013), nor to maintain maturation status of primary hepatocytes in culture (Fraczek et al., 2013). Future research is needed to elucidate pathways that are important for terminal differentiation of hepatocytes.

We compared several liver organoid species (mouse, human, dog, and cat), and in all observed lipid accumulation when liver organoids were provided with FFA. Oleate and palmitate represent the most abundant fatty acid species in healthy and steatotic human and cat liver (Araya et al., 2004; Fujiwara et al., 2015). Hence, oleate and palmitate are widely used in lipidomics research and are considered physiologically relevant for modeling hepatic lipid accumulation (Gómez-Lechón et al., 2007). Hepatocytes have three major routes to handle FFA. They can (1) enter β -oxidation to provide energy or a substrate for ketogenesis, or they can be re-esterified to triglycerides, and either (2) become excreted in very-low-density lipoproteins (VLDL) or (3) be stored as intracellular lipid droplets. There were marked species differences in the extent of lipid accumulation on a cellular level: feline liver organoids accumulated more lipids than did human liver organoids. This exaggerated phenotype of lipid overload in feline liver cells complies with the fact that steatosis in cats often leads to liver failure and severe disease (Center, 2005). We can speculate that the other metabolic pathways handling excess FFA (β -oxidation, VLDL secretion) are quickly saturated in feline hepatocytes, leading to extensive lipid-droplet formation. Both human and feline organoids upregulated *PLIN2* expression after FFA treatment, an essential machinery protein in lipid accumulation in lipid droplets. However, we also observed differences in transcriptional activation between human and feline organoids after FFA treatment, which could be explained by differences in activation of essential lipid regulatory pathways (mainly via PPARA and PPARG). Future research might focus on species differences in PPARA and PPARG signaling in response to excess FFA and their effects on hepatocellular lipid catabolism and storage.

To further explore the value of feline liver organoids as a research model for steatosis, we tested the effect of small molecules on lipid metabolism. Lipid accumulation was enhanced in the presence of etomoxir, indicating that β -oxidation is an important metabolic pathway handling excess fatty acids in feline liver cells. Conversely, supplementation of L-carnitine of feline liver organoids attenuated lipid accumulation in high-fat conditions and improved cellular viability. This is in concordance with the finding that exogenous L-carnitine supplementation can ameliorate FFA oxidation in cats with FHL (Center et al., 2012). The possibility to interfere in vitro with organoid lipid accumulation offers opportunities to test new drugs that enhance β -oxidation or promote VLDL secretion, with the aim of eliminating superfluous triglycerides from hepatocytes in vivo.

In conclusion, we describe a long-term three-dimensional primary culture of feline liver organoids, and demonstrate that they retain characteristics of adult liver



stem cells and are highly similar to liver organoids of other species. The pronounced phenotype of lipid accumulation in feline liver organoids compared with organoids from other species reveals remarkable species differences in cellular lipid-handling capacity. Hence, feline liver organoids represent an *in vitro* magnifying glass to investigate the molecular underpinnings of fatty liver disease and can become a valuable research tool to explore new therapeutic strategies for hepatic steatosis.

EXPERIMENTAL PROCEDURES

Liver Samples

Surplus liver samples were obtained postmortem from five cats (two female, three male); no animals were harmed or killed for the purpose of this study. Sample handling is further described in [Supplemental Experimental Procedures](#).

Mouse ($n = 4$ donors) and dog ($n = 4$ donors) liver organoid cultures were generated as described earlier from surplus liver material harvested from animals in non-liver-related research (experiments approved by the Utrecht University's ethical committee) ([Huch et al., 2013](#); [Nantasanti et al., 2015](#)).

Human ($n = 4$ donors) liver organoid cultures were generated as described earlier from surplus material of donor livers used for liver transplantations performed at the Erasmus Medical Center, Rotterdam (approved by the Medical Ethical Council of the Erasmus MC) ([Huch et al., 2015](#)).

Isolation of Biliary Ducts and Feline Liver Organoid Culture

Liver wedge biopsies were minced with scalpel blades and washed in DMEM medium with 1% (v/v) fetal calf serum and 1% (v/v) penicillin-streptomycin (all from Gibco). Samples were enzymatically digested with 0.3 mg/mL type II collagenase (Gibco) and 0.3 mg/mL dispase (Gibco) at 37°C for 2–3 hr and triturated every 20 min. Supernatant was checked for biliary duct fragments. Supernatant was centrifuged at $80 \times g$ for 5 min at 4°C and pelleted ducts were mixed with cold Matrigel (BD Biosciences). The FNA material was washed, but not minced nor digested before mixing with Matrigel. Matrigel suspension was seeded as droplets in 48- or 24-well plates and allowed to solidify at 37°C before overlaying with culture medium. Expansion medium as published for mouse, dog, and human liver organoids was tested on feline liver organoids ([Huch et al., 2013, 2015](#); [Nantasanti et al., 2015](#)). Medium effects on organoid proliferation were evaluated over the short term (1-week growth curve) with an Alamar blue assay according to the manufacturer's instructions (Life Technologies). Medium effects on organoid expansion in long-term culture were derived from weekly split ratios. Based on the obtained results (see also [Figure S1](#)), a new medium composition was developed (cat expansion medium [cEM]), which was a hybrid between dog and human expansion media. cEM consisted of Advanced DMEM/F12, supplemented with 1% (v/v) penicillin-streptomycin, 1% (v/v) GlutaMax, 10 mM HEPES (all Gibco), 2% (v/v) B27 minus vitamin A (Invitrogen), 1% N2 (Invitrogen), 10 mM nicotinamide (Sigma-Aldrich), 1.25 mM N-acetylcysteine (Sigma-Aldrich), 5% (v/v)

R-spondin-1 conditioned medium (the Rspo1-Fc-expressing cell line was a kind gift from Calvin J. Kuo), 10 μ M forskolin (Sigma-Aldrich), 10 μ M Y-27632 (ROCK inhibitor, Selleckchem), 0.5 μ M A83-01 (transforming growth factor β inhibitor, Tocris Bioscience), 50 ng/mL EGF (Invitrogen), 25 ng/mL HGF (Peprotech), 0.1 μ g/mL fibroblast growth factor 10 (Peprotech), 1 nM gastrin (Sigma-Aldrich), and 0.1 μ g/mL Noggin (Peprotech). Medium was changed every 2–3 days. Organoids were passaged by mechanical disruption once a week at an average split rate of 1:11. Imaging of the organoids was performed using an Olympus CKX41 microscope in combination with a Leica DFC425C camera.

Feline Liver Organoid Differentiation

Feline liver organoids of four donors in similar passage number (p5–p7) were cultured in cEM for 5 days, after which the medium composition was changed. In differentiation medium, nicotinamide, R-spondin-1, forskolin, and Y27632 were withdrawn and 25 ng/mL BMP7 (Peprotech), 10 μ M DAPT (γ -secretase inhibitor, Selleckchem), and 30 μ M dexamethasone (Sigma-Aldrich) were added. Differentiation medium was replaced every other day until the end of differentiation (day 7).

Measuring Lipid Accumulation in Liver Organoids with Flow Cytometry

Liver organoids of mouse, human, dog, and cat (four donors per species) were treated with either 0.4 mM oleate (C18:1) and 0.2 mM palmitate (C16:0) coupled to 12% (w/v) fatty acid-free BSA (all from Sigma-Aldrich) or with fatty acid-free BSA as vehicle control for 24 hr (details provided in [Supplemental Experimental Procedures](#)) and then dissociated to single cells with TrypLE select enzyme (Gibco). Cell suspensions were washed, and an aliquot was mixed with 0.4% trypan blue and counted on an automated cell counter (Bio-Rad). Cells were incubated with 0.025 μ g/mL LD450 (lipophilic dye, kindly provided by Christoph Thiele) for 30 min at 37°C. Incubations without LD540 served as a negative control. Cells were washed and resuspended in Hank's balanced salt solution with 5 nM Sytox red (Gibco). Cells were analyzed by flow cytometry on a FACSAria II SORP (BD Biosciences) ([Figure S1](#)). A 635-nm laser with an emission detection of 670/30 nm was used to detect Sytox red; dead cells were excluded from analysis. A 532-nm laser with emission detection at 610/20 nm was used to detect lipid accumulation in cells using LD540. The voltage was either 619 mV (Sytox red) or 300 mV (LD540).

SUPPLEMENTAL INFORMATION

Supplemental Information includes Supplemental Experimental Procedures, three figures, and two tables and can be found with this article online at <http://dx.doi.org/10.1016/j.stemcr.2017.02.015>.

AUTHOR CONTRIBUTIONS

Conceptualization, H.S.K., L.C.P., and B.S.; Methodology and Experiments, H.S.K., L.A.O., I.G.W.H.V., I.M.S., M.E.v.W., F.B., C.R., L.v.U., and M.R.M.; Data analysis and Interpretation, H.S.K., M.R.M., J.B.H., G.C.M.G., and B.S.; Writing, H.S.K., L.C.P., and



B.S.; Funding Acquisition, H.S.K. and B.S.; Resources, M.M.A.V., L.J.W.v.d.L., M.H., N.G., R.G.V., H.C., J.R., B.A.S., and L.C.P.

ACKNOWLEDGMENTS

The authors would like to thank the Utrecht University Center for Cell Imaging for technical assistance with imaging, Stefan van der Elst from the Hubrecht Institute for technical assistance with flow cytometry experiments, Dr. Sathidpak Nantasanti for technical advice, Dr. Hilda Toussaint for providing surplus mouse liver samples, and Sarah Opitz for editing the manuscript. This study was sponsored by the Winn Feline Foundation (grant no. W15-037). Parts of this work were funded by the Dutch Research Council NWO ZON/MW (116004121).

Received: September 5, 2016

Revised: February 17, 2017

Accepted: February 17, 2017

Published: March 23, 2017

REFERENCES

- Araya, J., Rodrigo, R., Videla, L.A., Thielemann, L., Orellana, M., Pettinelli, P., and Poniachik, J. (2004). Increase in long-chain polyunsaturated fatty acid n - 6/n - 3 ratio in relation to hepatic steatosis in patients with non-alcoholic fatty liver disease. *Clin. Sci. (Lond)* *106*, 635–643.
- Center, S.A. (2005). Feline hepatic lipidosis. *Vet. Clin. North Am. Small Anim. Pract.* *35*, 225–269.
- Center, S.A., Crawford, M.A., Guida, L., Erb, H.N., and King, J. (1993). A retrospective study of 77 cats with severe hepatic lipidosis: 1975-1990. *J. Vet. Intern. Med.* *7*, 349–359.
- Center, S.A., Warner, K.L., Randolph, J.F., Sunvold, G.D., and Vickers, J.R. (2012). Influence of dietary supplementation with (L)-carnitine on metabolic rate, fatty acid oxidation, body condition, and weight loss in overweight cats. *Am. J. Vet. Res.* *73*, 1002–1015.
- Cohen, J.C., Horton, J.D., and Hobbs, H.H. (2011). Human fatty liver disease: old questions and new insights. *Science* *332*, 1519–1523.
- Fraczek, J., Bolleyn, J., Vanhaecke, T., Rogiers, V., and Vinken, M. (2013). Primary hepatocyte cultures for pharmaco-toxicological studies: at the busy crossroad of various anti-dedifferentiation strategies. *Arch. Toxicol.* *87*, 577–610.
- Fujiwara, M., Mori, N., Sato, T., Tazaki, H., Ishikawa, S., Yamamoto, I., and Arai, T. (2015). Changes in fatty acid composition in tissue and serum of obese cats fed a high fat diet. *BMC Vet. Res.* *11*, 200.
- Gómez-Lechón, M.J., Donato, M.T., Martínez-Romero, A., Jiménez, N., Castell, J.V., and O'Connor, J.E. (2007). A human hepatocyte cellular in vitro model to investigate steatosis. *Chem. Biol. Interact.* *165*, 106–116.
- Huch, M., Dorrell, C., Boj, S.F., Van Es, J.H., Li, V.S., Van De Wetering, M., Sato, T., Hamer, K., Sasaki, N., Finegold, M.J., et al. (2013). In vitro expansion of single Lgr5+ liver stem cells induced by Wnt-driven regeneration. *Nature* *494*, 247–250.
- Huch, M., Gehart, H., Van Boxtel, R., Hamer, K., Blokzijl, F., Versteegen, M.M., Ellis, E., Van Wenum, M., Fuchs, S.A., De Ligt, J., et al. (2015). Long-term culture of genome-stable bipotent stem cells from adult human liver. *Cell* *160*, 299–312.
- Ijzer, J., Kisjes, J.R., Penning, L.C., Rothuizen, J., and Van Den Ingh, T.S.G.A.M. (2009). The progenitor cell compartment in the feline liver: an (immuno)histochemical investigation. *Vet. Pathol.* *46*, 614–621.
- Kruitwagen, H.S., Spee, B., Viebahn, C.S., Venema, H.B., Penning, L.C., Grinwis, G.C., Favier, R.P., van den Ingh, T.S.G.A.M., Rothuizen, J., and Schotanus, B.A. (2014). The canine hepatic progenitor cell niche: molecular characterisation in health and disease. *Vet. J.* *201*, 345–352.
- Nantasanti, S., Spee, B., Kruitwagen, H.S., Chen, C., Geijsen, N., Oosterhoff, L.A., Van Wolferen, M.E., Pelaez, N., Fieten, H., Wubolts, R.W., et al. (2015). Disease modeling and gene therapy of copper storage disease in canine hepatic organoids. *Stem Cell Rep.* *5*, 895–907.
- Ochiya, T., Yamamoto, Y., and Banas, A. (2010). Commitment of stem cells into functional hepatocytes. *Differentiation* *79*, 65–73.
- Roskams, T.A., Libbrecht, L., and Desmet, V.J. (2003). Progenitor cells in diseased human liver. *Semin. Liver Dis.* *23*, 385–396.
- Roskams, T.A., Theise, N.D., Balabaud, C., Bhagat, G., Bhathal, P.S., Bioulac-Sage, P., Brunt, E.M., Crawford, J.M., Crosby, H.A., and Desmet, V. (2004). Nomenclature of the finer branches of the biliary tree: canals, ductules, and ductular reactions in human livers. *Hepatology* *39*, 1739–1745.
- Sato, T., Vries, R.G., Snippert, H.J., Van De Wetering, M., Barker, N., Stange, D.E., Van Es, J.H., Abo, A., Kujala, P., Peters, P.J., et al. (2009). Single Lgr5 stem cells build crypt-villus structures in vitro without a mesenchymal niche. *Nature* *459*, 262–265.
- Wang, X., Foster, M., Al-Dhalimy, M., Lagasse, E., Finegold, M., and Grompe, M. (2003). The origin and liver repopulating capacity of murine oval cells. *Proc. Natl. Acad. Sci. USA* *100*, 11881–11888.
- Younossi, Z.M., Koenig, A.B., Abdelatif, D., Fazel, Y., Henry, L., and Wymer, M. (2016). Global epidemiology of nonalcoholic fatty liver disease—meta-analytic assessment of prevalence, incidence, and outcomes. *Hepatology* *64*, 73–84.
- Zhang, Z., Liu, J., Liu, Y., Li, Z., Gao, W.Q., and He, Z. (2013). Generation, characterization and potential therapeutic applications of mature and functional hepatocytes from stem cells. *J. Cell. Physiol.* *228*, 298–305.